Effects of Aerosol Solubility and Regeneration on Mixed-Phase Orographic Clouds and Precipitation

LULIN XUE,*,** AMIT TELLER,+ ROY RASMUSSEN,* ISTVAN GERESDI,# ZAITAO PAN,@ AND XIAODONG LIU&

* *National Center for Atmospheric Research, Boulder, Colorado*
+ *The Cyprus Institute, Nicosia, Cyprus*
# *University of Pécs, Pécs, Hungary*
@ *Saint Louis University, St. Louis, Missouri*
& *SKLLQG, Institute of Earth Environment, Chinese Academy of Sciences, Xi'an, China*

(Manuscript received 12 April 2011, in final form 29 November 2011)

ABSTRACT

A detailed bin aerosol-microphysics scheme has been implemented into the Weather Research and Forecast Model to investigate the effects of aerosol solubility and regeneration on mixed-phase orographic clouds and precipitation. Two-dimensional simulations of idealized moist flow over two identical bell-shaped mountains were carried out using different combinations of aerosol regeneration, solubility, loading, ice nucleation parameterizations, and humidity. The results showed the following. 1) Pollution and regenerated aerosols suppress the riming process in mixed-phase clouds by narrowing the drop spectrum. In general, the lower the aerosol solubility, the broader the drop spectrum and thus the higher the riming rate. When the solubility of initial aerosol increases with an increasing size of aerosol particles, the modified solubility of regenerated aerosols reduces precipitation. 2) The qualitative effects of aerosol solubility and regeneration on mixed-phase orographic clouds and precipitation are not affected by different ice nucleation parameterizations. 3) The impacts of aerosol properties on rain are similar in both warm- and mixed-phase clouds. Aerosols exert weaker impact on snow and stronger impact on graupel compared to rain as graupel production is strongly affected by riming. 4) Precipitation of both warm- and mixed-phase clouds is most sensitive to aerosol regeneration, then to aerosol solubility, and last to modified solubility of regenerated aerosol; however, the precipitation amount is mainly controlled by humidity and aerosol loading.

1. Introduction

Orographic clouds are important contributors to precipitation around the world and work as the central part of the interaction between the land surface and the atmosphere (Roe 2005). Natural hazards such as flash floods, landslides, and avalanches are affected by orographic precipitation. Recently, Levin and Cotton (2009) recommended more dedicated research efforts on observational and modeling campaigns aimed at studying the interaction of aerosol and precipitation in orographic clouds.

Observational studies (Borys et al. 2000, 2003) have showed that both riming and snowfall rates of mixed-phase orographic clouds are less when small cloud droplets are present as compared to large droplets. The source of the small droplets may be the result of high aerosol concentration produced by anthropogenic sources. A recent observational study by Lowenthal et al. (2011) explored the snow growth history by investigating oxygen isotopic ratios and sulfate concentrations in cloud water and snow collected at Storm Peak Laboratory during winter 2007. They found that riming rates of snow decrease sharply when the droplet mean diameter is less than 10 μm. Their results also indicated that snow growth by both riming and deposition occurred at low altitudes over long horizontal trajectories in the orographic flow upwind of the mountain crest. Therefore, anthropogenic aerosols might have important impacts on the distribution of precipitation in mountainous

** Current affiliation: National Center for Atmospheric Research, Boulder, Colorado.

Corresponding author address: Lulin Xue, National Center for Atmospheric Research, Boulder, CO 80301.
E-mail: xuel@ucar.edu

DOI: 10.1175/JAS-D-11-098.1

regions where snowpack is the main source of water for local populations.

Numerical study by Lohmann (2004) applied a size-dependent riming efficiency in a general circulation model to study the effect of anthropogenic aerosol on the riming process and the snowfall rate globally. The study revealed that the riming rate is reduced as a result of anthropogenic-aerosol-induced decreases in cloud droplet size. However, the increasing cloud life time reduces solar radiation that in turn increases the snowfall globally. More recently, Saleeby and Cotton (2008) and Lin and Colle (2011) applied different size-dependent riming approaches to orographic cloud simulations. Their results showed that significant improvements of snowfall prediction over mountainous areas have been achieved compared to size-independent riming approach. Muhlbauer et al. (2010) investigated the anthropogenic aerosol effects on mixed-phase orographic clouds by simulating an ideal two-dimensional bell-shaped case with three dynamic frameworks coupled with three state-of-the-art microphysical schemes. The intercomparison results indicated that, despite the variability in sensitivity among models, all models qualitatively agree on an overall decrease of orographic precipitation with an increase of aerosol concentration.

It has been shown by many recent modeling studies that an increase of anthropogenic aerosols not only impacts the precipitation amount on the ground but also changes the precipitation distribution over the mountainous regions (Lynn et al. 2007; Muhlbauer and Lohmann 2008; Saleeby et al. 2009; Muhlbauer et al. 2010; Saleeby et al. 2011). The reduced riming efficiency as the result of pollution produces more slow falling crystals that are transported downwind before reaching the ground (the so-called spillover effect). By running a bin microphysics scheme coupled with the Weather Research and Forecast Model (WRF) in a 2D setup, Lynn et al. (2007) found that pollutants suppress precipitation and shift the precipitation peak to the leeward slope. Saleeby et al. (2009) and Saleeby et al. (2011) applied the Regional Atmospheric Modeling System and a bulk microphysics scheme with bin-emulated riming treatment to simulate 3D real winter cases over the Colorado Rocky Mountain area in high resolution. They found that pollutants do not change the precipitation amount significantly domainwise but exert a great spillover effect that strongly impacts the water resource distribution in mountainous regions.

Besides their effect on mixed-phase microphysical processes through acting as cloud condensation nuclei (CCN), aerosol particles serving as ice nuclei (IN) are important for the ice initiation in orographic clouds (Targino et al. 2006; Mertes et al. 2007; Cozic et al. 2008). But, the extremely complicated behaviors of ice particles and insufficient measurements make the assumption of available IN as a function of meteorological conditions and available aerosol properties inconclusive. Although a recent report by DeMott et al. (2010) showed that a relation might exist between available IN and aerosol particles with diameter greater than 0.5 μm, the accurate representation of available IN in a numerical model is still challenging.

In a previous study (Xue et al. 2010b, hereafter X10), we have demonstrated that the release of aerosol particles to the atmosphere by evaporated clouds (aerosol regeneration) should be included in numerical models since it is a physical process in clouds and impacts simulated warm-phase orographic clouds and precipitation. The regeneration of CCN has been treated in numerical models for a long time (Hatzianastassiou et al. 1998; Wurzler et al. 2000; Saleeby and Cotton 2004; Yin et al. 2005). The regenerated CCN number is a prognostic variable in many models working as a source term in the CCN budget equation. In X10, not only the number concentration of regenerated aerosol is predicted, but also the solubility and size distribution of these aerosols are described. The different solubilities and size distributions of regenerated aerosol affect cloud and precipitation properties by altering the microphysical pathways. Based on their effects on warm-phase clouds, it is natural to extend the study to the potential impact of aerosol solubility and regeneration on mixed-phase orographic cloud and precipitation features.

Figure 1 illustrates such a scenario: the initial background aerosols consist of different chemical components (solubilities) with different sizes. These aerosols acting as both CCN and IN initiate mixed-phase clouds through drop activation and ice nucleation. Via various mixed-phase microphysical processes, these clouds produce precipitation in different forms such as freezing rain, snow, and graupel. At the same time, the aerosols that initiated these clouds interact with cloud hydrometeors. Some aerosols are scavenged by precipitation and some are released back into the air from sublimated ice particles and evaporated drops. These after-cloud-processing regenerated aerosols have different size distributions and solubilities than the initial aerosols. When the meteorological conditions are favorable, these regenerated aerosols activate new mixed-phase clouds with different cloud and precipitation properties than those in the first cycle.

Two-dimensional simulations of idealized cloud formation over two identical bell-shaped mountains have been carried out in this study to investigate the aerosol solubility and regeneration effect on mixed-phase orographic clouds and precipitation amount. The same detailed bin microphysics scheme implemented in WRF as

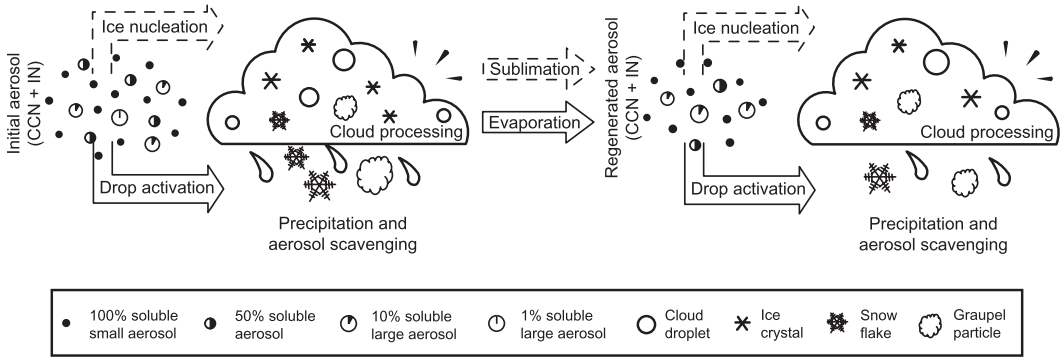

FIG. 1. Schematic diagram of the effects of aerosol solubility and regeneration on mixed-phase clouds and precipitation.

in X10 is applied in this study. Ideally, ice nucleation process is a function of local meteorological conditions and size distribution and chemical properties of the available aerosols. However, such a detailed ice nucleation parameterization is not available in this bin scheme. Therefore, we only examine the effects of aerosols acting as CCN, that is, aerosol effects on drop size distribution and its subsequent effects on mixed-phase orographic clouds and precipitation in this study (e.g., the solid-lined arrow chain in Fig. 1). Sensitivities of cloud properties and precipitation amount to ice nucleation parameterization, aerosol loading, and humidity are to be explored as well. We address the following research questions in this paper.

- How are mixed-phase microphysical processes especially riming process influenced by aerosol solubility and regeneration?
- Does the use of different ice nucleation parameterizations change the qualitative results of the previous questions?
- Are the impacts of aerosol on mixed-phase clouds stronger or weaker than those on warm-phase clouds?
- How sensitive are warm-phase and mixed-phase precipitation amount to aerosol properties and humidity?

The mixed-phase microphysics in this detailed bin scheme are described in section 2, and the experimental design is presented in section 3. The analyses and discussion of the results are provided in section 4, followed by the conclusions in section 5. The important spillover effect of pollution on orographic clouds will be investigated in a separated study.

2. Description of the mixed-phase detailed bin microphysical scheme

The detailed bin microphysics scheme used in this study applies the method of moments (Tzivion et al. 1987; Reisin et al. 1996; Geresdi 1998) to ensure the conservation of mass concentration (mixing ratio) and number concentration over 36 mass bins for the following species: water drops, pristine ice crystals, snowflakes, and graupel particles. Thirty-six mass doubling size bins covering a mass range of $1.598 \times 10^{-14} - 0.0011$ kg (1.56 μm − 6.4 mm in radius for water drops) are used to describe the evolution of the size distribution of each hydrometeor species. A detailed aerosol activation and regeneration submodule has been developed to predict the activation and regeneration of aerosol over 40 bins (radius range of 0.006−66.2 μm) with a certain solubility value in each bin. Besides the aerosol activation, regeneration, scavenging, and the warm-phase processes described in X10, the following mixed-phase microphysical processes are also simulated in this study.

1) Ice crystal formation by deposition and condensation freezing.
2) Ice crystal and graupel initialization by freezing of supercooled drops through immersion and contact freezing. If the radii of the drops are less than 50 μm, pristine ice crystals are formed. Larger drops become graupel particles.
3) Diffusion process (deposition and sublimation) of ice, snow, and graupel.
4) Melting of ice, snow, and graupel.
5) Collisions between pristine ice crystals and small water droplets result in snowflakes. If the mass of a water drop is greater than the pristine ice crystal, a graupel particle is formed.
6) Self-collisions of and collisions between pristine ice crystals and snowflakes increase snow mass.
7) Collisions between small water droplets and snowflakes result in snow growth if the diffusion growth of snow dominates the riming process; otherwise, graupel particles are formed. If the mass of a water drop is greater than the snowflake, a graupel particle is formed.

8) Collisions between water drops and graupel particles increase the mass of graupel.
9) Secondary ice formation of the Hallett–Mossop (H–M) process due to collisions between water drops and graupel particles.

The pristine ice crystals are assumed to have the form of a thin hexagonal plate. When the diffusion growth is calculated, this shape is approximated by an oblate spheroid with two different axes. The density of the pristine ice crystals is 900 kg m^{-3}. The diameter depends on the square root of the mass following Hobbs (1974). Terminal velocity is a linear function of the diameter (Hobbs 1974). The efficiency of drop–pristine ice collision–coalescence is given by parabolic functions fitted to the theoretical results of Pitter (1977). The collision efficiency of ice–ice aggregate changes linearly from zero to unity as the ice diameter increases from 20 to 100 μm. The corresponding coalescence efficiency depends on temperature (Lin et al. 1983).

The snowflake species is, for the most part, a combination of rimed ice crystals and snow aggregates. When the mass of a snowflake is small (less than 3.77×10^{-11} kg with the diameter of about 100 μm), an approximated shape of a hexagonal plate is assumed to represent that of rimed ice crystals. The density of small snowflakes is 900 kg m^{-3}. The terminal velocity depends on the diameter (Hobbs 1974). When the mass of a snowflake is large (greater than 2.23×10^{-8} kg with the diameter about 500 μm), a spherical shape is assumed to represent that of aggregates. The density of large snowflakes is 340 kg m^{-3}. Mass-based linear interpolations of axis ratio and density are applied to the snowflake with mass in between. The dependencies of the density and the terminal velocity on the size are based on Passarelli and Srivastava (1979). The efficiency of the drop–aggregate collision–coalescence depends linearly on the size of the drop from zero to unity as the diameter of the drop increase from 5 to 50 μm for small snowflakes and from 5 to 20 μm for larger ones. The collision efficiency of snow–snow aggregate and snowflake–ice aggregate is equal to unity and the coalescence efficiency depends on temperature (Lin et al. 1983).

Graupel particles are assumed to be of spherical symmetry. The density depends on the size, increasing linearly from 450 to 900 kg m^{-3} as its diameter increases from about 100 μm to 1 mm. The terminal velocity is given by Rasmussen and Heymsfield (1987). Collision efficiencies between water drops and graupel particles are calculated based on the table in Khain et al. (2001).

The Meyers (Meyers et al. 1992) and Cooper (Cooper 1986) parameterizations are applied in the scheme to initialize the ice crystals by deposition and condensation freezing. The immersion freezing rate is approximated by the Bigg parameterization (Bigg 1953) between 238 and 263 K. The Meyers parameterization is used for the contact freezing process. The formula suggested by Harris-Hobbs and Cooper (1987) is used to calculate the H–M secondary ice production. Aerosol particles released from the sublimated ice-phase particles are not considered in this study both because their concentrations are several orders of magnitude smaller than those released from the evaporated water drops and because the ice formation is not determined by available aerosols in this scheme.

3. Experimental design

Most of the model setups in this study are the same as X10 in which all mixed-phase microphysical processes were turned off (see X10 for details). The 2D domain consists of 400 grid points in the horizontal with a resolution of 2 km. There are 60 terrain-following vertical levels in the domain reaching the model top at 23 km. Two identical bell-shaped mountains are located at 200 and 500 km with peak height 800 m. The boundary layer physics, surface layer physics, and radiation are all turned off. Typical clean and polluted background aerosol concentrations consisting of three modes of lognormal distribution are prescribed. The number concentration of aerosol with radius greater than 0.05 μm is 73 cm^{-3} for the clean condition and 5659 cm^{-3} for the polluted condition. The soundings used to initialize the idealized 2D model are shown in Fig. 2. The solid line indicates the temperature and the dash lines indicate the dewpoint temperatures for two relative humidities (0.95 indicated by a long dashed line and 0.85 indicated by a short dashed line). The surface temperature is set to 273.15 K in this paper, which is different from 280.15 K as used in X10. The freezing ground temperature prevents an unrealistic high concentration of large drops as a result of instant shedding of water from melting ice-phase particles.

Based on the numerical findings that larger aerosol particles will be generated by orographic cloud processing (Xue et al. 2010a; Xue 2010) and different size distributions of regenerated aerosols have negligible effects on clouds and precipitation (X10), only a bimodal size distribution of regenerated aerosol particles (BMD1 as defined in X10) is used to simulate the regeneration effect on mixed-phase clouds and precipitation (see X10 for details). Besides solubility distributions of 100% (F1), 50% (F05), 10% (F01), and FC (solubility decreases with increasing aerosol radius representing mixtures of ammonia sulfate, anthropogenic pollution, and dust) described in X10, a new solubility distribution function (FCR) is added in this study to represent the

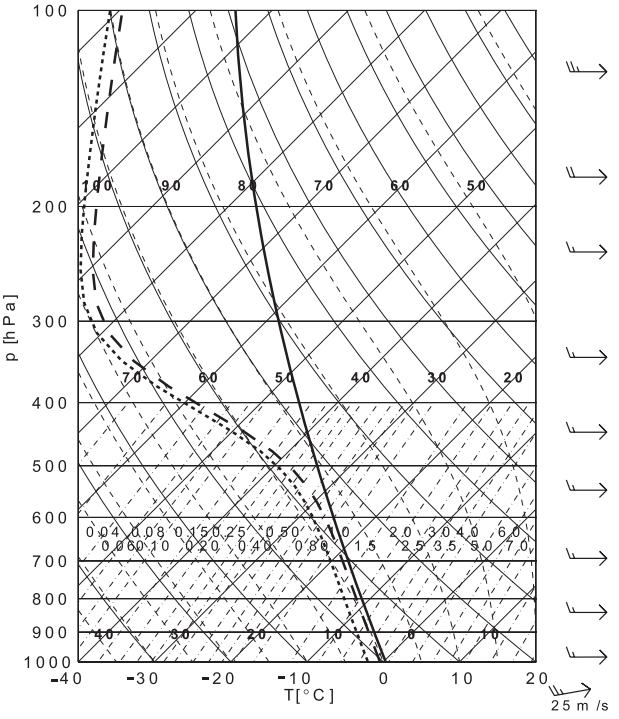

FIG. 2. Skew T–log$p$ plot of the atmospheric soundings for the ideal 2D simulations. The solid line indicates temperature; the dashed and dotted lines indicate dewpoint temperature. The surface temperature is 273.15 K. The surface relative humidity is 0.95 (dashed line) and 0.85 (dotted line). The wind speed is 15 m s^{-1} below 10 km and increases linearly to ~ 39 m s^{-1} at the domain top.

internal mixture of large soluble aerosol such as sea salt particles and small insoluble aerosol such as black carbon or soot particles:

$$\mathrm{FCR} = \begin{cases} 0.1, & r \le 5\times10^{-8} \\ 0.2, & 5\times10^{-8} < r \le 1\times10^{-6} \\ 0.5, & 1\times10^{-6} < r \le 5\times10^{-6} \\ 1, & r > 5\times10^{-6} \end{cases}. \quad (1)$$

Here r is the aerosol radius in meters. The effects of modified solubility of regenerated aerosol particles on clouds and precipitation are investigated by two groups of experiments. One is associated with FC in which the solubility of regenerated aerosols greater than 0.05 μm is assigned to 0.1 for the clean condition and 0.5 for the polluted condition. The other is associated with FCR with solubility of regenerated aerosol particles greater than 0.05 μm assigned to 0.5 for both clean and polluted clouds (as FCR_F05 cases).

Table 1 summarizes all the simulations that have been carried out using the Meyers ice nucleation parameterization in this study. All experiments were repeated using the Cooper parameterization to test whether the sensitivities are independent of the different ice nucleation methods. The regeneration of aerosol is not considered in the CTRL cases. Each case has been simulated for 10 h.

TABLE 1. List of experiments and their notations.[a]

Case/solubility	F1	F05	F01	FC	FCR
			Wet clean		
C_RH95_CTRL	×[b]	×	×	×	×
C_RH95_BMD1	×	×	×	×[c]	×[c]
			Dry clean		
C_RH85_CTRL	×[b]	×	×	×	×
C_RH85_BMD1	×	×	×	×[c]	×[c]
			Wet polluted		
P_RH95_CTRL	×[b]	×	×	×	×
P_RH95_BMD1	×	×	×	×[c]	×[c]
			Dry polluted		
P_RH85_CTRL	×[b]	×	×	×	×
P_RH85_BMD1	×	×	×	×[c]	×[c]

[a] The "C" and "P" stand for the clean and polluted background, respectively. "RH95" and "RH85" indicate the wet and dry condition. "CTRL" has no regenerated aerosol. A cross indicates a combining case has been performed. All experiments are repeated using the Cooper parameterization.
[b] Additional cases using the sounding in the warm-phase study.
[c] Additional cases for modified solubility of regenerated aerosol particles as described in the text.

4. Results and discussion

a. *Effects of aerosol solubility and regeneration on clouds and precipitation over the second hill*

Figure 3 illustrates the time-averaged mixing ratios of cloud water (color-shaded areas), rainwater (black lines), ice (green lines), snow (yellow lines), and graupel (red lines). All contour lines start at 0.01 g kg^{-1} with an interval of 0.1 g kg^{-1}. The freezing temperature (0°C) and cloud-top temperature (−25°C) are indicated by the bottom and top white lines, respectively. The scheme simulated a mixed-phase orographic cloud on the upstream side of the mountain and an upper-level orographic wave cloud in a region of wave breaking on the leeward side of the mountain. Supercooled liquid water reaches about 0.5 g kg^{-1} in each case, which makes these clouds sensitive to aerosol properties. There is little pristine ice content in the orographic clouds because the efficient riming and ice–ice collision processes in these clouds convert most pristine ice crystals into snow. Snow consists of the majority of the orographic cloud, reaching 0.5 g kg^{-1} in most cases.

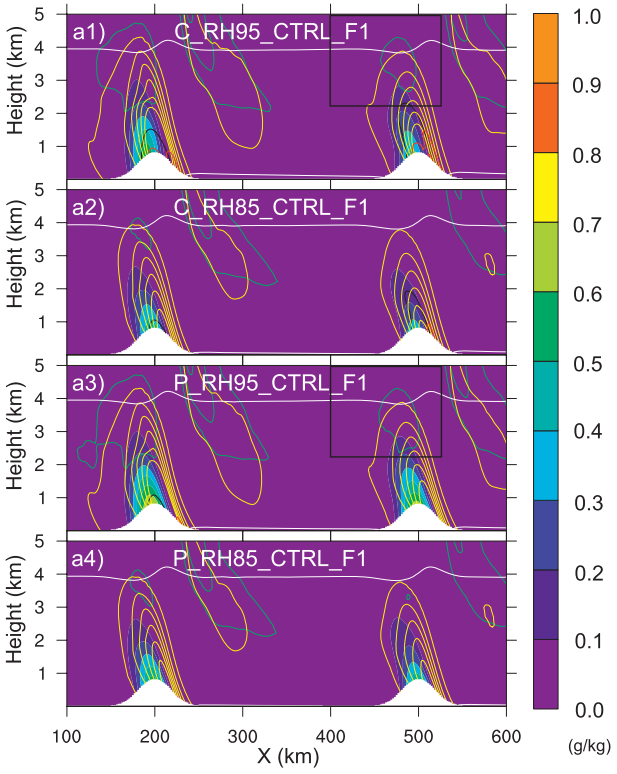

FIG. 3. Time-averaged cloud, rain, ice, snow, and graupel mixing ratios (g kg^{-1}) (T_{sfc} = 273.15 K) in the lowest 5 km of the domain. The color-shaded areas represent cloud water. The black, green, yellow, and red contours represent rain, ice, snow, and graupel content, respectively. All contour lines start at 0.01 g kg^{-1} with an interval of 0.1 g kg^{-1}; the 0°C temperature is indicated by the white line at the bottom and the white line on the top represents cloud-top temperature of −25°C. The black boxes in (a1) and (a3) indicate the areas based on which the time series were calculated as shown in Fig. 6.

In this study, we focus on the aerosol–cloud–precipitation interactions of the orographic cloud over the second hill (not the wave cloud), which are affected by regenerated aerosols. The cloud properties, precipitation features, mixed-phased microphyscal processes, and their interactions will be analyzed in the following sections.

1) CLOUD PROPERTIES AND PRECIPITATION FEATURES

Since aerosol regeneration is a physical process that should be represented in numerical models, we plot the properties of clouds generated by different aerosol solubilities with regeneration (BMD1 cases) in Figs. 4 and 5. The time series of total mass and number of water drops, ice crystals, snowflakes, and graupel particles together with the associated rain, snow, and graupel domain-averaged precipitation rates are plotted for clean and polluted clouds over the second hill, respectively. Unless mentioned otherwise, results of simulations using the Meyers parameterization are analyzed hereafter.

Similar to warm-phase clouds, the number of water drops in mixed-phase clouds is sensitive, while the water mass is insensitive to aerosol loading and solubility. The impacts of aerosol solubility on cloud drops and rain rate are more significant in polluted clouds than in clean clouds, which agrees qualitatively well with the findings in X10 (Figs. 4a1,b1, and c1 and Figs. 5a1,b1, and c1). Through the same mechanism demonstrated in X10 for warm-phase clouds, aerosol solubility determines the concentrations of CCN and giant CNN (GCCN) under the same aerosol loading and leads to different drop size distributions in mixed-phase clouds (see Fig. 8).

Unlike cloud water drops, cloud ice crystals and snowflakes are not as sensitive to the aerosol loading. The magnitudes and time series of mass, number, and precipitation rate are very similar in clean and polluted clouds for ice[1] and snow species. Both ice and snow show some sensitivities to aerosol solubility before 4 h. The different responses between ice/snow and water to aerosol loading and solubility are partially due to the fact that the ice initialization in the scheme is decoupled with the aerosol properties.

Graupel, on the other hand, is very sensitive to aerosol loading and solubility owing to its formation mechanism, which requires collisions of ice-phase particles and large water drops. The total mass, number, and precipitation rate of graupel species are greater in clean clouds than in polluted clouds. At the same time, they vary greatly with aerosol solubility in both clean and polluted clouds.

The ground accumulations of rain, snow, and graupel over the second hill at the end of all simulations are listed in Table 2. Although the majority of the precipitation on the ground is in ice-phase (snow and graupel), there is still a fair amount of supercooled liquid precipitation on the ground. Comparisons between warm-phase and mixed-phase simulations showed that the surface rain increases with a decreasing solubility in general except that 100% aerosol solubility generated more rain than 50% solubility in polluted clouds (see Tables 2 and 5).

For FC cases, the solubility of regenerated aerosols decreases in the radius range of 0.05 to 1 μm and increases for particles greater than 1 μm. The reduced solubility of the majority of the CCN population activates fewer but larger cloud droplets, leading to more rain on the ground (asterisk rows in Table 2), in agreement with

[1] The ice falling on the ground is classified as snow precipitation in this scheme.

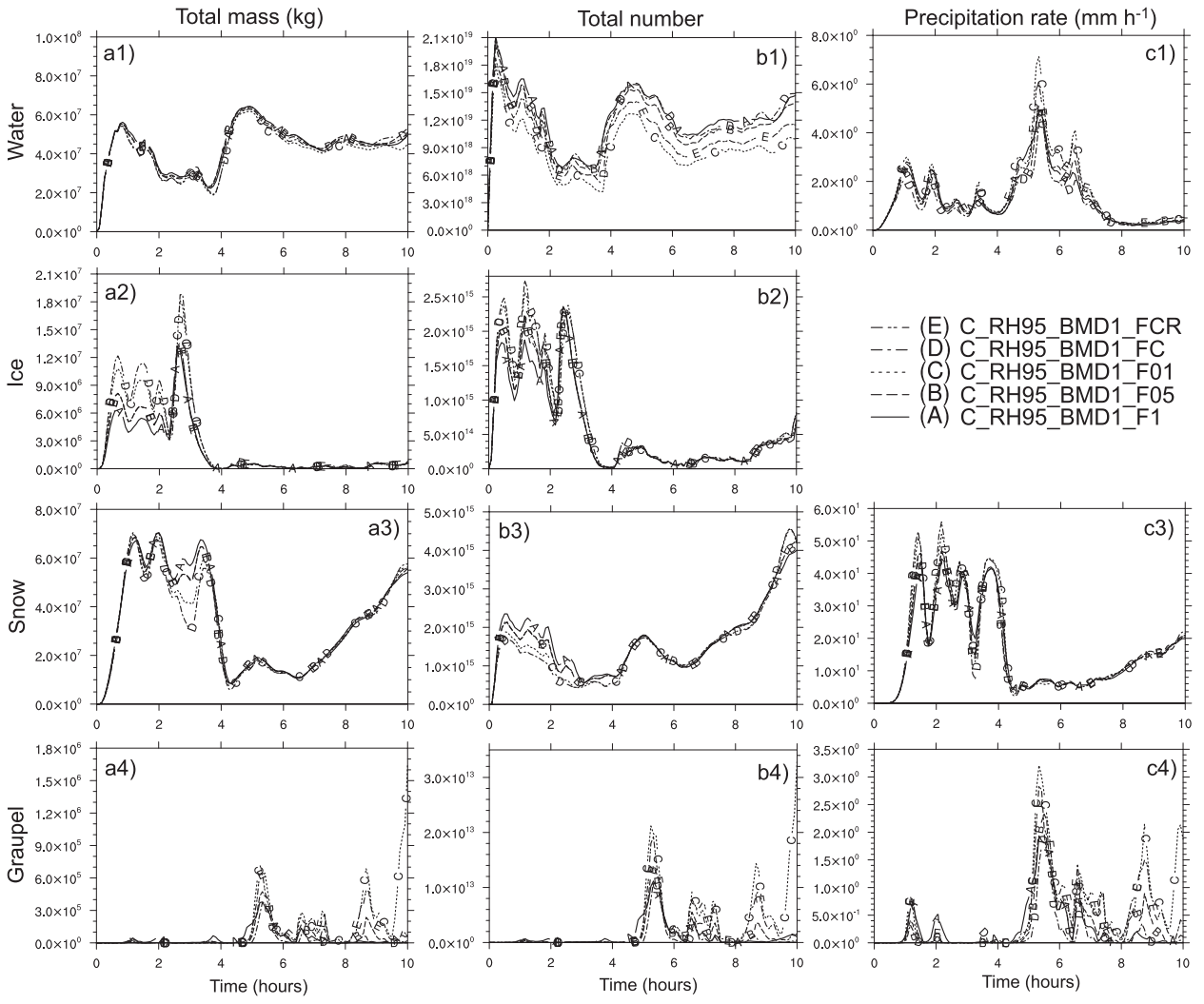

FIG. 4. Time series of (a) total mass of cloud water, ice, snow, and graupel (kg); (b) total number of cloud drops, ice crystals, snowflakes, and graupel particles; and (c) precipitation rates (mm h^{-1}) of rain, snow, and graupel for C_RH95_BMD1 cases. Lines A–E represent solubility functions of F1, F05, F01, FC, and FCR, respectively.

X10. On the other hand, the increased aerosol solubility of regenerated aerosols between 0.05 and 1 μm generated less rain in FCR cases. This result echoes the point made in X10 that, if the aerosol solubility distribution is very different from FC, such as FCR, the impact on precipitation could be reversed.

Snow on the ground is similar to ice and snow in the cloud, which is not very sensitive to aerosol concentration, solubility, and regeneration. Snow on the ground tends to increase with decreasing aerosol solubility. Because the growing mechanisms of snow involving deposition, aggregation, and riming are quite different from that of rain, which is mainly controlled by collision–coalescence, snow does not change the same way as the rain does when the solubility of regenerated aerosol was modified for the FC and FCR cases.

Graupel amount on the ground is lower than rain and snow and is most sensitive to aerosol concentration, solubility, regeneration, and humidity among all precipitation types. There is practically no graupel on the ground from polluted clouds. In these orographic clouds, graupel grows mainly through coagulations of ice-phase particles and large drops, which is similar to the growth mechanism of rain. Therefore, graupel on the ground reproduces the same trend as rain in most cases.

The macrophysical properties of mixed-phase clouds and precipitation showed that different hydrometeors respond to aerosol properties differently. These responses of mixed-phase clouds are also very different from those of warm-phase clouds. Analyses of mixed-phase microphysical processes, especially riming process, affected by aerosols in next section will reveal these differences.

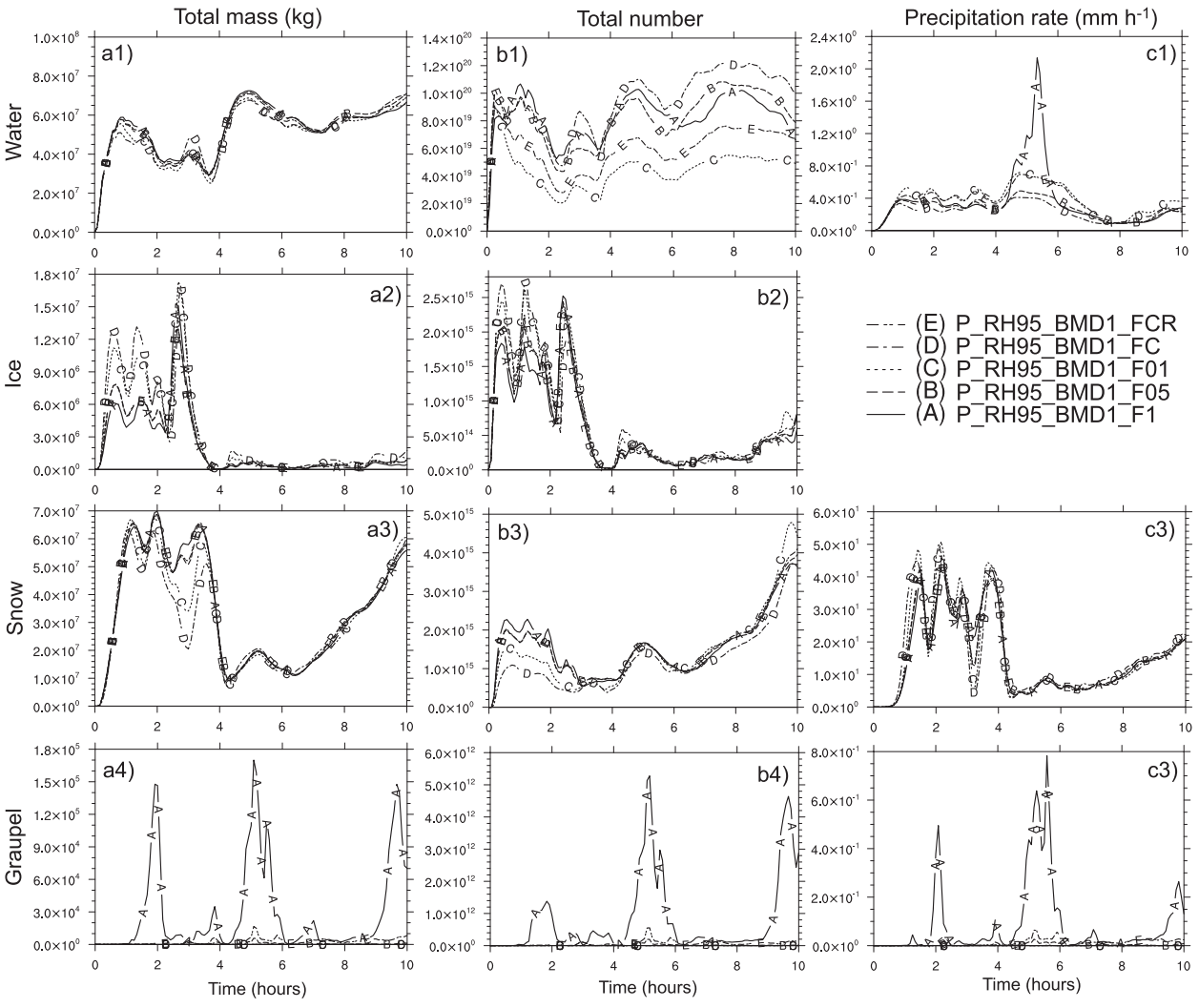

FIG. 5. As in Fig. 4, but for the P_RH95_BMD1 cases.

2) AEROSOL EFFECTS ON THE RIMING PROCESS

The Meyers parameterization predicts IN concentrations based on the supersaturation ratio over ice. It is found that the time series of maximum ice saturation ratios and available water vapor within the black boxes where the majority of primary ice crystals were formed (shown in Fig. 3) are basically the same for the C_RH95_BMD1 and P_RH95_BMD1 cases (Figs. 6a,b). This feature implies that the dynamics of the mixed-phase orographic clouds investigated here is insensitive to aerosol properties. Therefore, the ice crystal number concentrations and mass mainly controlled by ice nucleation and diffusion growth are insensitive to aerosol properties (see Figs. 4a2,b2 and 5a2,b2).

The time series of the integrated mass converting rates (kg s^{-1}) of water collected by ice (defined as riming rate by ice) and ice mass involved in riming process (defined as ice converting rate by riming) in the same boxed region are plotted in Figs. 6c,d. Both variables show distinct patterns in the 0–4-h and 4–10-h periods. Time- and space-averaged drop and ice crystal size distributions (cm^{-3} μm^{-1}) of these periods are plotted in Figs. 6e–h. The vertical lines indicate the threshold values (10 μm for drop and 160 μm for ice) above which riming of ice is active (Pitter 1977).

In the period 0–4 h, the active riming process is the result of interactions between newly nucleated crystals and activated drops in this region (see the high supersaturation over ice in this period in Fig. 6a). In this activation stage, large aerosols dominate the drop size spectrum. Cases with higher solubility associated with large aerosols produce wider spectra than others. In both clean and polluted clouds, F1 cases generated most

TABLE 2. Ground total precipitation (mm) for clouds over the second hill from all sensitivity cases using the Meyers parameterization for ice nucleation.

	Rain (mm)					Snow (mm)					Graupel (mm)				
Case/solubility	F1	F05	F01	FC	FCR	F1	F05	F01	FC	FCR	F1	F05	F01	FC	FCR
								Wet clean							
C_RH95_CTRL	28	28	26	25	29	154	157	162	164	155	26	27	25	24	30
C_RH95_BMD1	13	13	16	11	15	160	163	169	171	162	2.7	2.8	5.4	1.5	4.5
*	—	—	—	12	14	—	—	—	171	163	—	—	—	4.0	3.2
								Dry clean							
C_RH85_CTRL	12	12	12	11	13	108	108	109	111	107	6.1	7.1	6.9	6.3	10.3
C_RH85_BMD1	5.1	5.1	5.9	4.9	5.4	103	104	107	106	105	0.15	0.03	0.21	0.01	0.09
*	—	—	—	5.3	5.3	—	—	—	108	104	—	—	—	0.06	0.05
								Wet polluted							
P_RH95_CTRL	3.6	2.7	4.0	2.5	3.5	153	153	160	162	154	0.80	0.03	0.00	0.00	0.06
P_RH95_BMD1	3.6	2.7	3.8	2.4	3.5	152	153	160	162	153	0.87	0.04	0.00	0.00	0.12
*	—	—	—	2.6	3.2	—	—	—	158	153	—	—	—	0.02	0.07
								Dry polluted							
P_RH85_CTRL	1.4	1.4	2.1	1.2	1.6	98	97	101	109	97	0.18	0.00	0.00	0.00	0.01
P_RH85_BMD1	1.5	1.3	2.0	1.2	1.6	97	97	101	111	97	1.3	0.01	0.00	0.00	0.01
*	—	—	—	1.2	1.4	—	—	—	105	97	—	—	—	0.01	0.01

* The values of cases with modified solubility of regenerated aerosol particles.

large drops ($r > 10$ μm) and FC cases form least large drops (Fig. 6e). At the same time, both clouds have very similar number of large ice crystals ($r > 160$ μm) for all solubilities (Fig. 6f). Therefore, the riming rates by ice correspond with drop size distributions (Figs. 6c,e). Unlike clean clouds, the concentrations of large drops are lower than those of large ice crystals in the F01 and FC cases under polluted conditions (curves C and D in Figs. 6e2 and f2). Thus, the ice converting rates of these two cases are limited by the available large drops, which are reflected in Fig. 6d2).

In the later period, 4–10 h, the declining water vapor controlled by the mountain wave suppresses the activation and nucleation processes (Figs. 6a,b). The available drops are those transported upward from the main cloud body below this region. Riming rates by ice are still in good agreement with the large drop concentrations. Unlike the earlier period, the ice converting rates are regulated by the available large ice crystals[2] because the number of large drops are always greater than that of large ice crystals in both clean and polluted clouds.

The time series of riming rates by snow and total number of large drops are illustrated in Figs. 7a1 and c1. Similar to riming of ice, snowflakes and large drops coagulate efficiently (see section 2). Therefore, good agreement between the riming rate by snow and concentration of large drops exists. The higher concentrations of large drops in F01 and FCR cases are attributed to their low solubility associated with small aerosols, which reduces the CCN concentration and shifts the small mode of drop spectrum toward the larger end (see Fig. 8c). Because snowflakes are initially formed by riming of ice crystals that are nucleated at high altitude, the snow amount is partially determined by the available ice crystals. We have demonstrated in previous analyses that there are more ice crystals being nucleated during the first 4-h period than the last 6-h period. Consequently, fewer snowflakes in the later period limit the riming efficiency even though the concentration of large drops is still high.

Production rates of graupel by riming of graupel, ice, and snow are plotted in Figs. 7a2,b1, and b2. As described in section 2, the collision–coalescence coefficient between ice-phase particles and water drops reaches unity when the radii of drops are greater than 50 μm and coagulations between ice-phase particles and such big drops usually result in graupel particles. Therefore, close correlation between graupel production rates and number of drizzle drops ($r > 50$ μm) is found (Fig. 7c2). It was found in X10 that under the polluted condition only the case of 100% solubility can activate enough large drops to initiate an efficient collision–coalescence process. Thus, a relatively high concentration of drizzle drops is only shown in curve A of Fig. 7c2.

[2] Notice that the slightly wider spectrum of curve D in Fig. 6d2 has the same implication as the slightly higher ice converting rate by riming as showed in the time series of curve D in Fig. 6h2.

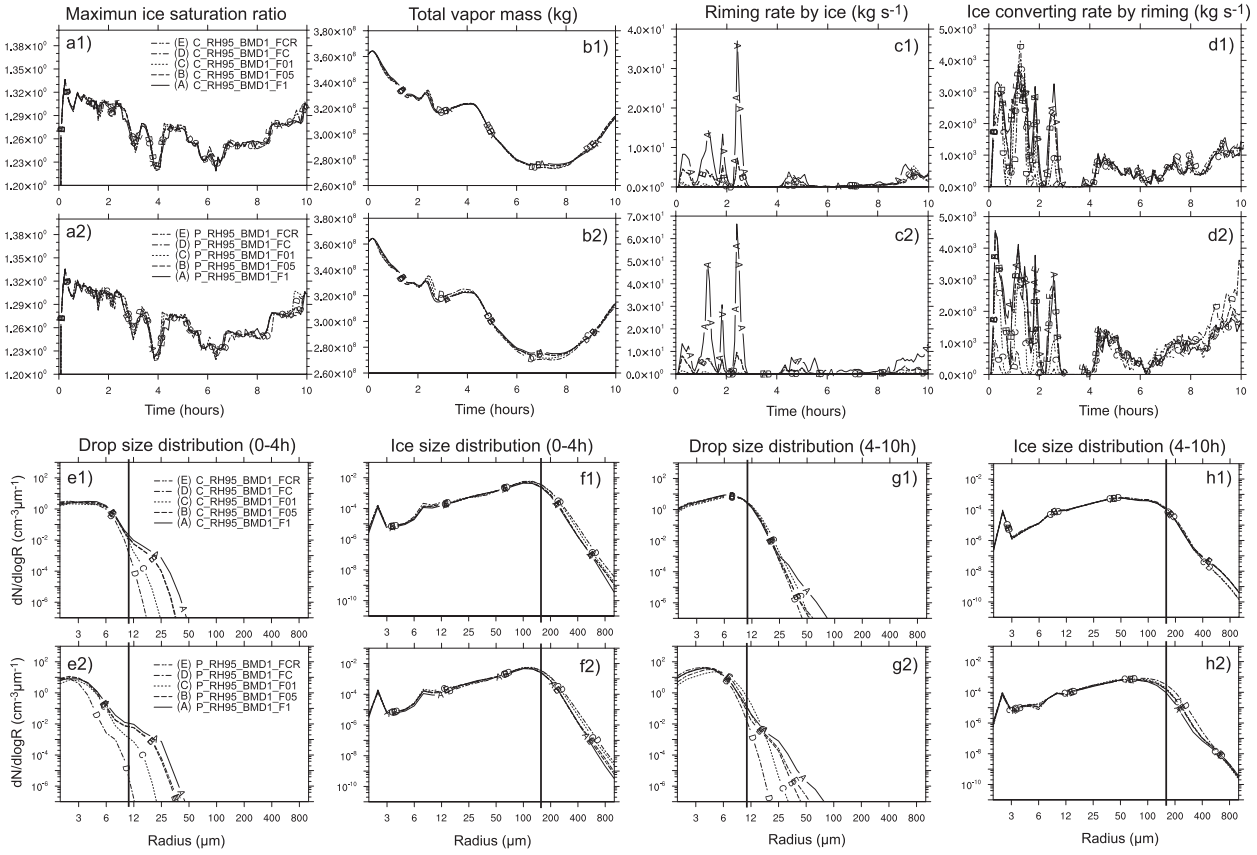

FIG. 6. Time series of (a) maximum ice saturation ratio, (b) total water vapor (kg), (c) riming rate by ice (kg s^{-1}), (d) ice converting rate by riming (kg s^{-1}), and (e) averaged drop size distribution over 0–4 h. (f) As in (e), but for ice. (g) As in (e), but for 6–10 h. (h) As in (f), but for 6–10 h for C_RH95_BMD1 and P_RH95_BMD1 cases. All time series were calculated within the areas indicated by the black boxes at the top in Figs. 3a1 and a3. Vertical lines indicate a radius of (e),(g) 10 and (f),(g) 160 μm.

Figure 8a shows the difference of water collected by ice, snow, and graupel (defined as the riming rate by ice-phase particles) between clean and polluted clouds for all solubility functions under a high humidity condition. This plot represents the effect of aerosol loading on the riming process. It clearly shows that pollution suppresses riming regardless of the aerosol solubility throughout the simulations. It is noticed from discussions in previous paragraphs that the riming by snow dominates that by ice and graupel (see Figs. 6c and 7a). Therefore, consistently lower concentrations of large drops in polluted clouds compared to clean clouds lead to this suppression (Figs. 8b,c). The suppression of the riming process by pollution was also found under low humidity condition (not shown).

Figures 8d,e illustrate the averaged size distributions of graupel particles in clean and polluted clouds under a high humidity condition. It is found that, in general, graupel size is larger under the clean condition. However, when aerosol is 100% soluble (F1), polluted clouds generated more large graupel particles ($r > 800$ μm) than in all clean clouds. This feature is attributed to the fact that the coalescence coefficients between graupel particles with radii greater than 320 μm and drops with radius range of 5–10 μm are comparable to those of larger drops (Khain et al. 2001). Therefore, given the similar amount of graupel particles greater than 320 μm in both clean and polluted clouds (Fig. 8d and curve A in Fig. 8e), the more small droplets ($r \leq 10$ μm) in polluted clouds lead to more large graupel particles than in clean clouds. Similar results have been found by Teller and Levin (2006) and Khain et al. (2011).

The analyses performed so far in this section have explored how aerosol solubility (F1 to FCR) and loading (clean vs polluted) affect the riming process. We now briefly demonstrate how aerosol regeneration (CTRL vs BMD1) and modified solubility of regenerated aerosol (FCR vs FCR_F05) impact the riming process. Figure 9 depicts the time series of riming rate by ice species, total number of large drops, and total number of drizzle drops

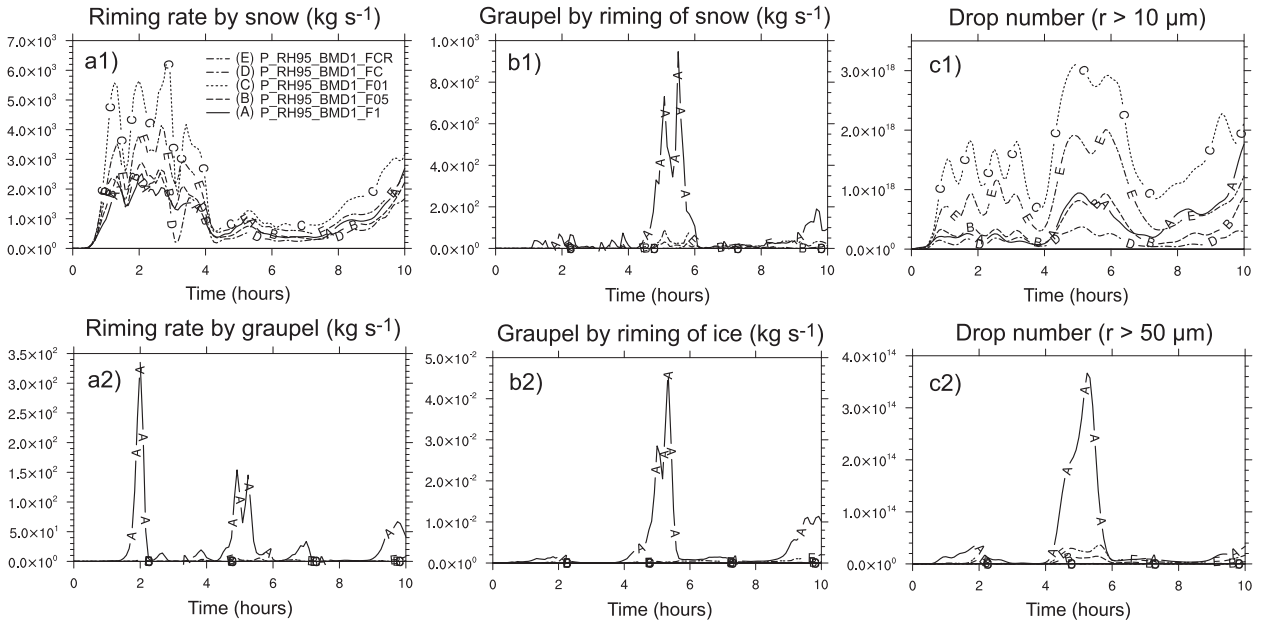

FIG. 7. Time series of (a) riming rate by snow and graupel (kg s^{-1}), (b) graupel production rate by riming of snow and ice (kg s^{-1}), and (c) total number of drops with radii greater than 10 and 50 μm for P_RH95_BMD1 cases.

for FCR cases (CTRL_FCR, BMD1_FCR, and BMD1_FCR_F05) under high humidity condition for both clean and polluted clouds.

It is obvious that without regenerated aerosols the second cloud become much cleaner by activating the interstial aerosols advected from the first cloud after 5 h. More large drops are present in the polluted CTRL case, which leads to a higher riming rate than others. Under clean conditions, the very low concentration of interstitial aerosols makes the condensation so efficient that

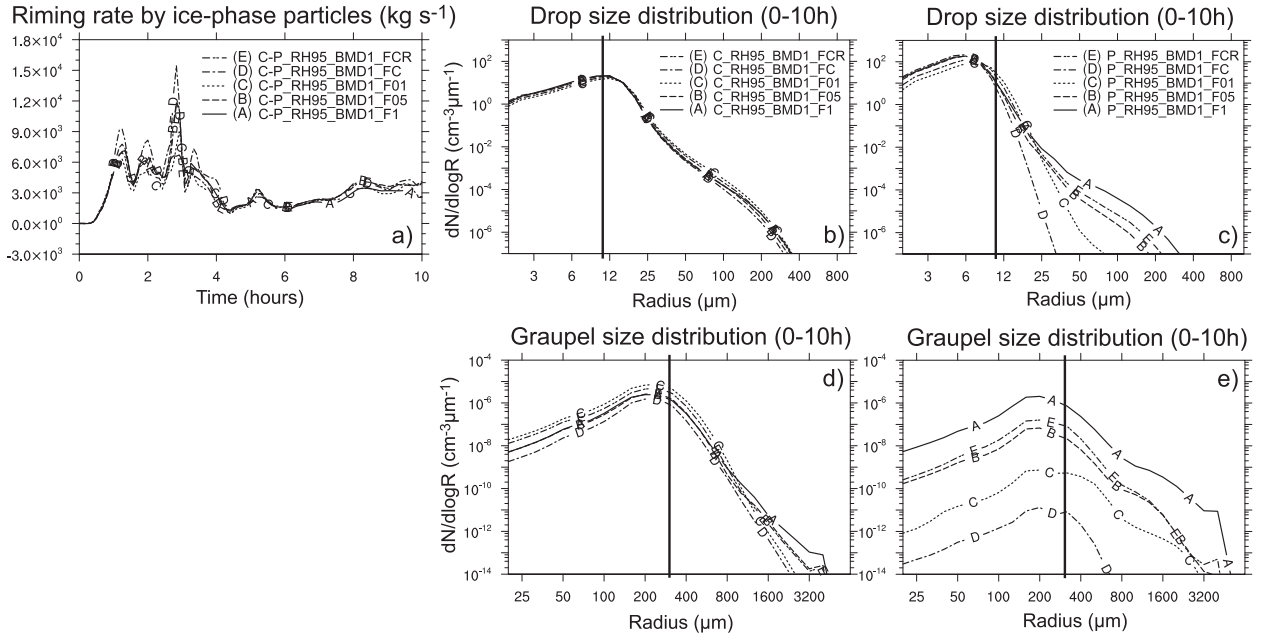

FIG. 8. Time series of (a) difference of riming rate by ice-phase particles between C_RH95_BMD1 and P_RH95_BMD1 cases (kg s^{-1}); (b),(d) time- and space-averaged drop and graupel size distributions of C_RH95_BMD1 cases; and (c),(e) time- and space-averaged drop and graupel size distributions of P_RH95_BMD1 cases. Vertical lines indicate a radius of (b),(c) 10 and (d),(e) 320 μm.

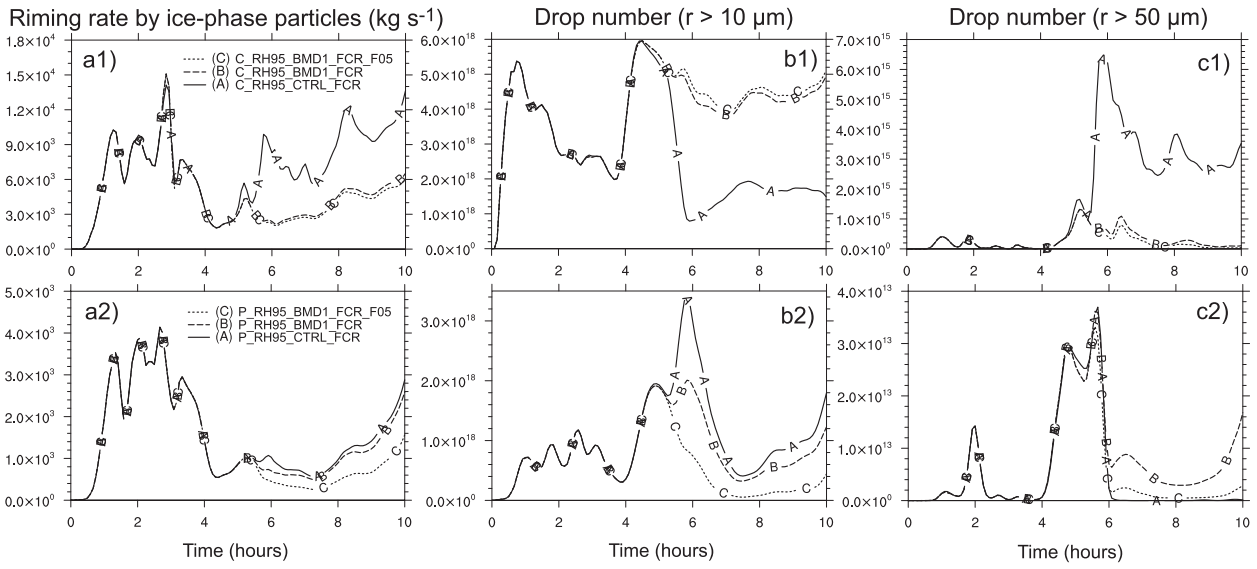

FIG. 9. Time series of (a) riming rate by ice-phase particles (kg s^{-1}), (b) total number of drops with radius greater than 10 μm, and (c) total number of drops with radius greater than 50 μm for FCR cases.

a significant amount of drizzle drops is formed. Even the concentration of large drops is lower in clean CTRL; these drizzle drops dominate the riming rate. For cases with aerosol regeneration (BMD1_FCR and BMD1_FCR_F05), the regenerated aerosol particles activated more drops than CTRL cases after 5 h under both clean and polluted conditions. BMD1_FCR_F05 cases had more drops activated than BMD1_FCR cases (drop number with $r \leq 10$ μm is not showed) due to the higher solubility of cloud-processed aerosol particles less than 1 μm [0.5 vs less equal than 0.5, see section 3 and Eq. (1)], which leads to more CCN. However, for giant aerosols ($r > 5$ μm), the BMD1_FCR_F05 cases have lower solubility than the BMD1_FCR cases (0.5 vs 1), which means that BMD1_FCR has more GCCN. Therefore, BMD1_FCR cases generate more drizzle drops in clean clouds and more large/drizzle drops in polluted clouds, and consequently more active riming process (Figs. 9a,c).

Although the riming process is the key in converting water mass into ice mass, diffusion (deposition and sublimation) is the dominant process in determing the mass of ice and snow under weak dynamics. Since diffusion is a function of particle surface area and it scales with the mass of an ice crystal or a nonaggregate snowflake owing to its plate shape (see section 2), the diffusion growth rates of these species are proportional to their mass, which is one or more orders of magnitude greater than the production rates of other microphysical processes. Because of the spherical shape of graupel particles, the diffusion process of graupel is not as active as that of ice and snow and thus riming is the most important process for graupel production.

Through detailed investigations of riming process, the effects of aerosol solubility and regeneration on mixed-phase orographic clouds simulated by the bin microphysical scheme with the Meyers parameterization have been explored in this section. As in warm-phase clouds, initial size distribution of drops in mixed-phase clouds are directly controlled by aerosol properties, especially aerosol loading. Ice initialization is not a direct function of aerosol properties but one of the dynamics, which is not sensitive to aerosol in this study. The similar number and mass of ice nucleated in all cases determined the big picture of ice and snow. Riming rates of ice and snow are proportional to drop concentration greater than 10 μm in radius, which is affected by aerosol loading, solubility, and regeneration. Graupel formation is proportional to drop concentration greater than 50 μm in radius, which is more sensitive to aerosol properties than those greater than 10 μm. Summaries of aerosol effect on the riming process are listed in Table 3.

3) EFFECTS OF ICE NUCLEATION PARAMETERIZATIONS

To find out whether the qualitative effects of aerosol solubility and regeneration on mixed-phase orographic clouds are affected by the ice nucleation parameterizations, the complete set of sensitivity experiments, as listed in Table 1, was conducted using the Cooper ice nucleation parameterization.

TABLE 3. Riming efficiency as a function of drop size radius r affected by aerosol properties.*

Condition/drop size	$r < 5$ μm	$5 \le r \le 10$ μm	$10 \le r < 50$ μm	r ≥ 50 μm
Riming efficiency	No riming	Low	High	Very high
Regeneration	+*	+	+/−	+/−
Pol–Cln	+	+	−	−
F05–F1 (Cln)	−	−	+	−
F01–F1 (Cln)	−	−	+	+
F05–F1 (Pol)	−	−	+	−
F01–F1 (Pol)	−	−	+	−

* The pluses and minuses indicate relative concentration change for certain drop size range. "Pol" and "Cln" stand for polluted and clean conditions.

Comparisons between Fig. 10 and Fig. 3 reveal that the Cooper parameterization generated more liquid water (cloud water reaches higher altitude), less ice and snow (fewer contour lines), and more graupel (broader area covered by the red contours) than the Meyers parameterization. These features were also reflected in Table 4. There is more rain, more graupel, and less snow on the ground for the Cooper runs. The explanation of these differences lies on the different IN concentrations predicted by these parameterizations. Figure 11 clearly shows that above −25°C, the cloud top temperature in this study, the Cooper parameterization consistently initializes less ice crystals than the Meyers at water saturation. Fewer ice crystals in the cloud compete for vapor less intensively with water drops and collect much less water than in the Meyers case, which in turn lead to more water, less ice, and less snow. It is further found that less active riming in the Cooper case contributes more than the less active diffusion to the water difference between the Meyers and the Cooper parameterization (not showed), in agreement with Rasmussen et al. (2002). As discussed in the previous section, graupel formation is approximately a function of drizzle drop concentration. Therefore the Cooper cases generate more graupel than the Meyers cases.

Similar analyses as performed in previous section reveal that the Cooper parameterization generates similar microphysical features to those simulated by the Meyers parameterization. Despite the quantitative differences of precipitation amount between these two parameterizations, Table 4 also shows similar effects of aerosol solubility and regeneration on mixed-phase precipitation amount to those of the Meyers cases.

b. *Sensitivities of precipitation to aerosol properties and humidity*

One important question to be addressed in this study is what are the sensitivities of mixed-phase orographic clouds properties and precipitation amount to aerosol characteristics and humidity compared to warm-phase clouds. In this section, we use ground precipitation data over the second hill (Tables 2, 4, and 5) to investigate this question. Table 5 is the same as Table 2, but for the rain from the warm-phase simulations using sounding with $T_{sfc} = 280.15$ K. Columns F1 to FC duplicated those from Table 4 in X10. To make comparison between warm-phase and mixed-phase precipitation complete we conducted warm-phase simulations with FCR solubility distribution and listed the rain data in this table.

We define five sensitivity parameters (SP) to represent the sensitivities of precipitation to different aerosol properties and humidity:

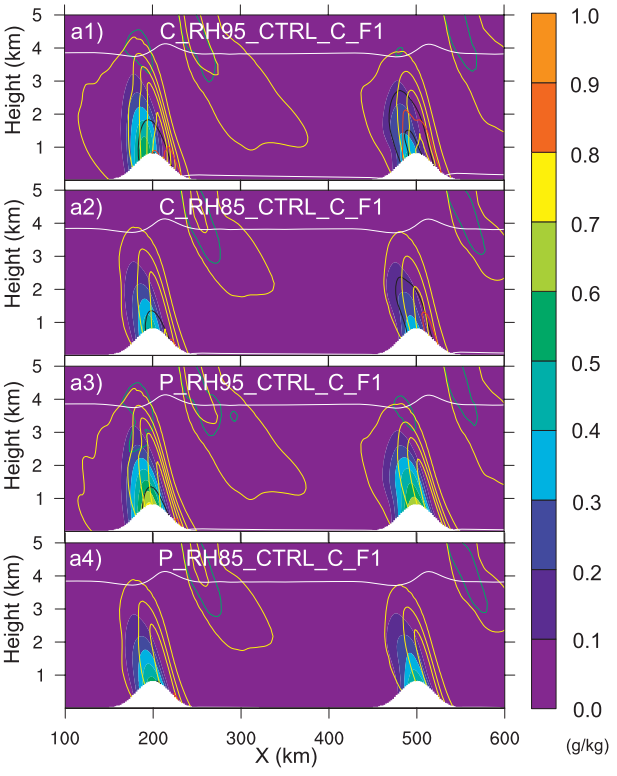

FIG. 10. As in Fig. 3, but for simulations with the Cooper parameterization.

TABLE 4. As in Table 2, but for simulations using the Cooper parameterization for ice nucleation.

	Rain (mm)					Snow (mm)					Graupel (mm)				
Case/solubility	F1	F05	F01	FC	FCR	F1	F05	F01	FC	FCR	F1	F05	F01	FC	FCR
								Wet clean							
C_RH95_CTRL	84	83	75	77	82	92	94	103	111	93	36	39	32	26	44
C_RH95_BMD1	35	38	45	26	45	98	100	104	114	98	16	16	20	11	19
*	—	—	—	37	40	—	—	—	112	99	—	—	—	16	17
								Dry clean							
C_RH85_CTRL	30	33	31	31	35	55	56	60	61	55	13	15	14	15	18
C_RH85_BMD1	7.1	6.8	9.1	6.3	7.9	59	61	64	66	61	0.36	0.48	2.5	0.21	1.2
*	—	—	—	7.5	7.2	—	—	—	66	61	—	—	—	1.3	0.58
								Wet polluted							
P_RH95_CTRL	4.8	3.3	5.7	3.0	4.5	103	106	114	116	107	0.83	0.06	0.31	0.00	0.16
P_RH95_BMD1	5.2	3.3	4.9	2.9	4.7	103	106	114	116	107	1.6	0.14	0.13	0.00	0.29
*	—	—	—	3.1	3.9	—	—	—	114	107	—	—	—	0.05	0.18
								Dry polluted							
P_RH85_CTRL	1.7	1.6	2.5	1.4	1.9	55	56	61	65	56	0.22	0.01	0.00	0.00	0.01
P_RH85_BMD1	1.7	1.5	2.2	1.4	1.9	54	56	60	65	56	0.26	0.02	0.00	0.00	0.05
*	—	—	—	1.5	1.6	—	—	—	64	56	—	—	—	0.01	0.02

$$
\begin{aligned}
SP_{\text{regeneration}} &= [(P_{\text{CTRL}} - P_{\text{BMD1}})/\max(P_{\text{CTRL}}, P_{\text{BMD1}})]_{|\text{loading,humidity}} \\
SP_{\text{solubility}} &= [(\max(P_{\text{FX}}) - \min(P_{\text{FX}})/\max(P_{\text{FX}})]_{|\text{regeneration}} \\
SP_{\text{mod-sol}} &= [P_{\text{FC}(R)-\text{F05}} - P_{\text{FC}(R)}]/\max[P_{\text{FC}(R)-\text{F05}}, P_{\text{FC}(R)}] \\
SP_{\text{loading}} &= [(P_{\text{cln}} - P_{\text{pol}})/\max(P_{\text{cln}}, P_{\text{pol}})]_{|\text{humidity,regeneration}} \\
SP_{\text{humidity}} &= [(P_{\text{wet}} - P_{\text{dry}})/\max(P_{\text{wet}}, P_{\text{dry}})]_{|\text{loading,regeneration}}.
\end{aligned} \tag{2}
$$

Here P is precipitation amount on ground in different types, FX indicates all solubility distributions, and cln and pol are for clean and polluted conditions. Each parameter is conditionally calculated. By these definitions, all SP range from −1 to 1, which is convenient to plot and compare with each other. We do not claim that these parameters are the best statistical indices to quantitatively or accurately represent the sensitivity of precipitation to those properties. We use these simple parameters to present the qualitative comparisons, despite the different surface temperature used in the warm-phase study.

Figure 12 shows the box or whisker plots of these five parameters. Different precipitation types are separated by dashed lines. Each box with lines consists of a series of data in which the box covers the 25th–75th percentiles, the lines reach minimum and maximum of the dataset, and the solid triangle represents the median. For example, in Fig. 12a the box over the Wet Pol column in the Warm Rain section consist of five values from all solubility cases under wet and polluted conditions. Each box in the mixed-phase regions consists of values from both the Meyers and the Cooper simulations because similar sensitivities have been found for the Meyers and the Cooper simulations.

It is noticed that regeneration effects on warm rain and mixed rain are similar except that mixed rain is not sensitive under the wet polluted condition (Fig. 12a). This insensitivity indicates that the riming process is limited by the available large drops under such condition. Aerosol solubility, modified solubility of regenerated aerosol, and aerosol loading impact rain of warm- and mixed-phase clouds in similar ways. The slightly higher sensitivity of mixed rain to aerosol loading than warm rain reflects that most of the large drops in polluted clouds are collected by ice-phase particles, which leads to a small amount of rain on the ground and thus a greater difference of rain between polluted and clean conditions. Humidity regulates the warm rain on the ground under all kinds of aerosol properties. The interactions between drops and ice-phase particles mitigate this effect of rain in mixed-phase clouds, but it is still very prominent.

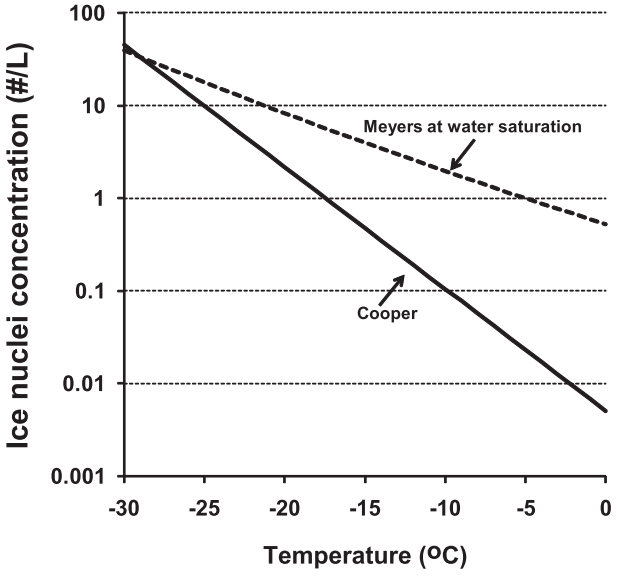

FIG. 11. Deposition and condensation ice nuclei concentration (L^{-1}) predicted by the Meyers and the Cooper parameterizations.

TABLE 5. As in Table 2, but for warm-phase clouds.

	Rain (mm)				
Case/solubility	F1	F05	F01	FC	FCR
			Wet clean		
C_RH95_CTRL	163	166	172	168	168
C_RH95_BMD1	99	108	144	95	130
*	—	—	—	117	118
			Dry clean		
C_RH85_CTRL	46	47	44	47	48
C_RH85_BMD1	15	15	20	14	18
*	—	—	—	18	16
			Wet polluted		
P_RH95_CTRL	53	66	102	51	84
P_RH95_BMD1	30	21	75	11	53
*	—	—	—	14	40
			Dry polluted		
P_RH85_CTRL	2.5	2.8	4.5	2.3	3.6
P_RH85_BMD1	2.5	2.7	4.0	2.2	3.7
*	—	—	—	2.4	2.8

Snow is not sensitive to all aerosol properties partly because ice nucleation is decoupled with aerosol properties and because the diffusion growth dominates the riming process in terms of snow production. The relatively strong dependence of snow on humidity confirms that dynamically determined IN concentration and diffusion growth control snow production, but the sensitivity of snow to humidity is lower than that of warm rain.

Graupel is more sensitive than warm rain to most aerosol properties due to its production related to drizzle drop concentration in clouds. Because the absolute amount of graupel on ground is very small in many cases, broad sensitivity ranges are observed in these plots. The regeneration effects on graupel from polluted clouds are opposite to those on warm rain because most of the large drops in these clouds contribute to the riming process of snow rather than graupel. The humiditiy effect on graupel is similar to that of warm rain.

Humidity determines the available water content of an orographic cloud and hence determines the available precipitation on the ground. Because extreme clean and extreme polluted conditions were used in this study, the aerosol loading effect on precipitation is very strong. For less extreme conditions, weaker aerosol loading effects are expected. Aerosol regeneration and solubility have similar sensitivities, which demonstrate that these effects should be included in numerical simulations of clouds. Although the modified solubility of regenerated aerosol shows lowest sensitivity, it is not trivial. Inclusion of this effect in numerical model is suggested.

5. Conclusions

The effects of solubility and regeneration of aerosol acting as CCN on clouds and precipitation have been evaluated by simulating 2D idealized mixed-phase cloud formation over two bell-shaped mountains using a detailed bin microphysical scheme embedded in the Weather Research and Forecasting Model (X10). Detailed investigations have shown how the riming process, mixed-phase clouds, and precipitation were affected by aerosol properties through changing the water drop size distribution. The qualitative sensitivity of mixed-phase clouds and precipitation to ice nucleation has been investigated using the Meyers and the Cooper parameterizations. Comparisons of sensitivity parameters between warm- and mixed-phase precipitation amount have been conducted, despite the different surface temperatures used in these two studies. The main conclusions of this aerosol–cloud–precipitation interactions study are summarized as follows.

1) Pollution and regenerated aerosols suppress the riming process in mixed-phase clouds by narrowing the drop spectrum. In general, the lower the aerosol solubility, the broader the drop spectrum and thus the higher the riming rate. Larger graupel particles are formed in polluted cloud compared to clean cloud when aerosol is 100% soluble, while a more than 50% reduction of ground graupel relative to the clean case is observed under the wet condition. When the solubility of initial aerosol increases with an increasing size of aerosol particles, the modified

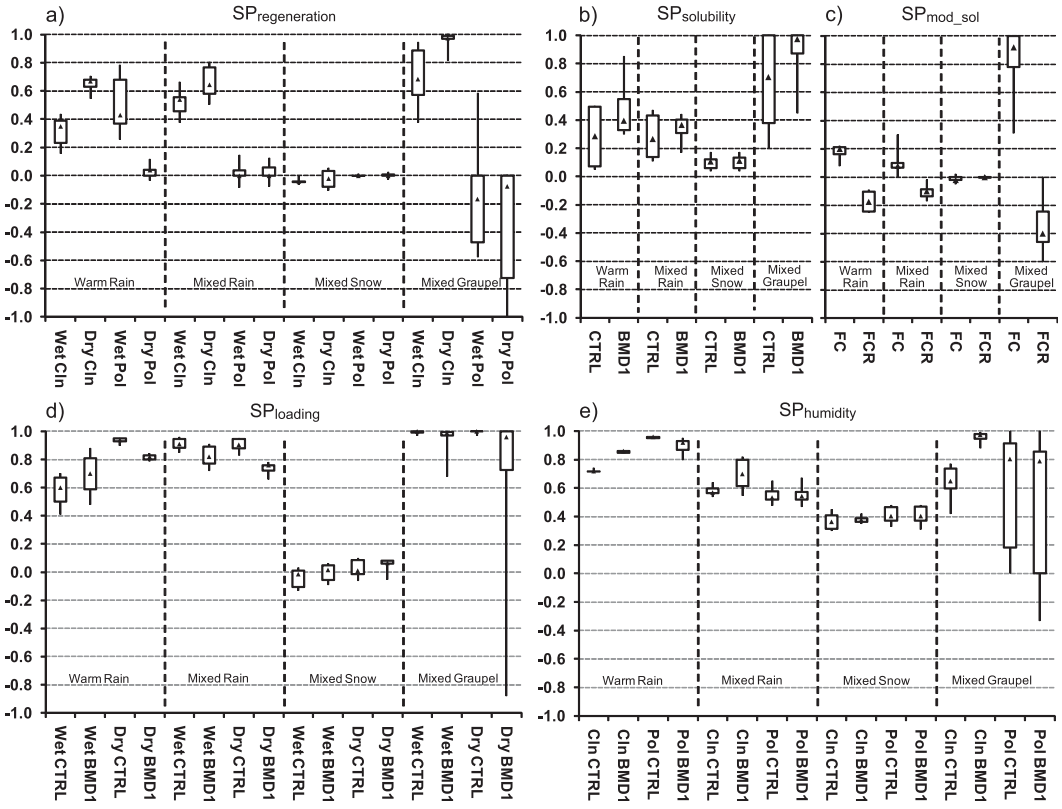

FIG. 12. Whisker plot of sensitivity parameter of (a) aerosol regeneration, (b) aerosol solubility, (c) modified aerosol solubility, (d) aerosol loading, and (e) humidity.

solubility of regenerated aerosol decreases the precipitation amount over the second mountain.

2) The Cooper parameterization simulated more rain, less snow, and more graupel than the Meyers parameterization, but the qualitative effects of aerosol solubility and regeneration on mixed-phase orographic clouds and precipitation are not affected by ice nucleation parameterizations.
3) The impacts of aerosol properties on rain are similar in both warm- and mixed-phase clouds. Aerosols exert a weaker impact on snow and a stronger impact on graupel compared to rain as graupel production is strongly affected by riming.
4) Precipitation of both warm- and mixed-phase clouds is most sensitive to aerosol regeneration, then to aerosol solubility, and last to a modified solubility of regenerated aerosol; however, the precipitation amount is mainly controlled by humidity and aerosol loading.

Both quantitative differences of precipitation between the Meyers and the Cooper simulations and that snow is insensitive to aerosol properties indicate that the accurate prediction of amount and phase partition of precipitation requires better knowledge of the linkage between ice nucleation and aerosol properties. Better understanding of aerosol–cloud–precipitation interactions in mixed-phase orographic clouds can be achieved by using models with such an ice nucleation approach.

Acknowledgments. This study was partly supported by the NCAR Advanced Study Program and the Wyoming Weather Modification Pilot Program. Geresdi was supported by the grant of Developing Competitiveness of Universities in the South Transdanubian Region (SROP-4.2.1.B-10/2/KONV-2010-0002). Pan was supported by NOAA Grant NA11OAR4310094. Liu is supported by the National Basic Research Program of China (2011CB403406). The authors are very grateful for the helpful comments and suggestions of the anonymous reviewers, which significantly improved this manuscript.

REFERENCES

Bigg, E. K., 1953: The formation of atmospheric ice crystals by the freezing of droplets. *Quart. J. Roy. Meteor. Soc.,* **79,** 510–519.

Borys, R., D. Lowenthal, and D. Mitchell, 2000: The relationships among cloud microphysics, chemistry, and precipitation rate in cold mountain clouds. *Atmos. Environ.,* **34,** 2593–2602.

——, ——, S. Cohn, and W. Brown, 2003: Mountaintop and radar measurements of anthropogenic aerosol effects on snow growth

and snowfall rate. *Geophys. Res. Lett.,* **30,** 1538, doi:10.1029/2002GL016855.

Cooper, W. A., 1986: Ice initiation in natural clouds. *Precipitation Enhancement—A Scientific Challege, Meteor. Monogr*., No. 21, Amer. Meteor. Soc., 29–32.

Cozic, J., and Coauthors, 2008: Chemical composition of free tropospheric aerosol for PM1 and coarse mode at the high alpine site Jungfraujoch. *Atmos. Chem. Phys.,* **8,** 407–423.

DeMott, P. J., and Coauthors, 2010: Predicting global atmospheric ice nuclei distributions and their impacts on climate. *Proc. Natl. Acad. Sci. USA,* **107** (25), 11 217–11 222.

Geresdi, I., 1998: Idealized simulation of the Colorado hailstorm case: Comparison of bulk and detailed microphysics. *Atmos. Res.,* **45,** 237–252.

Harris-Hobbs, R. L., and W. A. Cooper, 1987: Field evidence supporting quantitative predictions of secondary ice production rates. *J. Atmos. Sci.,* **44,** 1071–1082.

Hatzianastassiou, N., W. Wobrock, and A. I. Flossmann, 1998: The effects of cloud-processing of aerosol particles on clouds and radiation. *Tellus,* **50B,** 478–490.

Hobbs, P. V., 1974: *Ice Physics*. Oxford Press, 837 pp.

Khain, A., M. Pinsky, M. Shapiro, and A. Pokrovsky, 2001: Collision rate of small graupel and water drops. *J. Atmos. Sci.,* **58,** 2571–2595.

——, D. Rosenfeld, A. Pokrovsky, U. Blahak, and A. Ryzhkov, 2011: The role of CCN in precipitation and hail in a mid-latitude storm as seen in simulations using a spectral (bin) microphysics model in a 2D dynamic frame. *Atmos. Res.,* **99,** 129–146.

Levin, Z., and W. R. Cotton, 2009: *Aerosol Pollution Impact on Precipitation*. Springer, 386 pp.

Lin, Y., and B. A. Colle, 2011: A new bulk microphysical scheme that includes riming intensity and temperature-dependent ice characteristics. *Mon. Wea. Rev.,* **139,** 1013–1035.

Lin, Y.-L., R. Farley, and H. D. Orville, 1983: Bulk parameterization of the snow field in a cloud model. *J. Climate Appl. Meteor.,* **22,** 1065–1092.

Lohmann, U., 2004: Can anthropogenic aerosols decrease the snowfall rate? *J. Atmos. Sci.,* **61,** 2457–2468.

Lowenthal, D. H., R. D. Borys, W. Cotton, S. Saleeby, S. A. Cohn, and W. J. Brown, 2011: The altitude of snow growth by riming and vapor deposition in mixed-phase orographic clouds. *Atmos. Environ.,* **45,** 519–522.

Lynn, B., A. Khain, D. Rosenfeld, and W. L. Woodley, 2007: Effects of aerosols on precipitation from orographic clouds. *J. Geophys. Res.,* **112,** D10225, doi:10.1029/2006JD007537.

Mertes, S., and Coauthors, 2007: Counterflow virtual impact or based collection of small ice particles in mixed-phase clouds for the physico-chemical characterization of tropospheric ice nuclei: Sample description and first case study. *Aerosol Sci. Technol.,* **41,** 848–864.

Meyers, M. P., P. J. DeMott, and W. R. Cotton, 1992: New primary ice-nucleation parameterization in an explicit cloud model. *J. Appl. Meteor.,* **31,** 708–721.

Muhlbauer, A., and U. Lohmann, 2008: Sensitiviy studies of the role of aerosol in warm-phase orographic precipitation in different dynamical flow regimes. *J. Atmos. Sci.,* **65,** 2522–2542.

——, T. Hashino, L. Xue, A. Teller, U. Lohmann, R. M. Rasmussen, I. Geresdi, and Z. Pan, 2010: Intercomparison of aerosol-cloud-precipitation interactions in stratiform orographic mixed-phase clouds. *Atmos. Chem. Phys. Discuss.,* **10,** 10 487–10 550.

Passarelli, R. E., and R. Srivastava, 1979: A new aspect of snowflake aggregation theory. *J. Atmos. Sci.,* **36,** 484–493.

Pitter, R. L., 1977: A reexamination of riming on thin ice plates. *J. Atmos. Sci.,* **34,** 684–685.

Rasmussen, R. M., and A. J. Heymsfield, 1987: Melting and shedding of hail and graupel. Part I: Model physics. *J. Atmos. Sci.,* **44,** 2754–2763.

——, I. Geresdi, G. Thompson, K. Manning, and E. Karplus, 2002: Freezing drizzle formation in stably stratified layer clouds: The role of radiative cooling of cloud droplets, cloud condensation nuclei, and ice initiation. *J. Atmos. Sci.,* **59,** 837–860.

Reisin, T., Z. Levin, and S. Tzivion, 1996: Rain production in convective clouds as simulated in an axisymmetric model with detailed microphysics. Part I: Description of the model. *J. Atmos. Sci.,* **53,** 497–519.

Roe, G. H., 2005: Orographic precipitation. *Annu. Rev. Earth Planet. Sci.,* **33,** 645–671.

Saleeby, S. M., and W. R. Cotton, 2004: A large-droplet mode and prognostic number concentration of cloud droplets in the Colorado State University Regional Atmospheric Modeling System (RAMS). Part I: Module descriptions and supercell test simulations. *J. Appl. Meteor.,* **43,** 182–195.

——, and ——, 2008: A binned approach to cloud-droplet riming implemented in a bulk microphysics model. *J. Appl. Meteor. Climatol.,* **47,** 694–703.

——, ——, D. Lowenthal, R. D. Borys, and M. A. Wetzel, 2009: Influence of cloud condensation nuclei on orographic snowfall. *J. Appl. Meteor. Climatol.,* **48,** 903–922.

——, ——, and J. D. Fuller, 2011: The cumulative impact of cloud droplet nucleating aerosols on orographic snowfall in Colorado. *J. Appl. Meteor. Climatol.,* **50,** 604–625.

Targino, A. C., R. Krejci, K. J. Noone, and P. Glantz, 2006: Single particle analysis of ice crystal residuals observed in orographic wave clouds over Scandinavia during INTACC experiment. *Atmos. Chem. Phys.,* **6,** 1977–1990.

Teller, A., and Z. Levin, 2006: The effects of aerosols on precipitation and dimensions of subtropical clouds: A sensitivity study using a numerical cloud model. *Atmos. Chem. Phys.,* **6,** 67–80.

Tzivion, S., G. Feingold, and Z. Levin, 1987: An efficient numerical solution to the stochastic collection equation. *J. Atmos. Sci.,* **44,** 3139–3149.

Wurzler, S., T. G. Reisin, and Z. Levin, 2000: Modification of mineral dust particles by cloud processing and subsequent effect on drop size distributions. *J. Geophys. Res.,* **105,** 4501–4512.

Xue, L., 2010: Externally mixed aerosols to internally mixed aerosols: A numerical study of cloud processing using a bin aerosol-microphysics scheme coupled with WRF. *Eos, Trans. Amer. Geophys. Union,* (Fall Meeting Suppl.), Abstract A13A-0177.

——, I. Geresdi, and R. Rasmussen, 2010a: Cloud processing of internal mixed aerosol: A numerical study using a bin aerosol-microphysics scheme coupled with WRF. Preprints, *13th Conf. on Cloud Physics,* Portland, OR, Amer. Meteor. Soc., 2.2. [Available online at http://ams.confex.com/ams/pdfpapers/170624.pdf.]

——, A. Teller, R. M. Rasmussen, I. Geresdi, and Z. Pan, 2010b: Effects of aerosol solubility and regeneration on warm-phase orographic clouds and precipitation simulated by a detailed bin microphysical scheme. *J. Atmos. Sci.,* **67,** 3336–3354.

Yin, Y., K. S. Carslaw, and G. Feingold, 2005: Vertical transport and processing of aerosols in a mixed-phase convective cloud and the feedback on cloud development. *Quart. J. Roy. Meteor. Soc.,* **131,** 221–245.